A new limit of the ^{129}Xenon Electric Dipole Moment

Fabian Allmendinger[1], *Ilhan* Engin[2], *Olivier* Grasdijk[3], *Werner* Heil[4], *Klaus* Jungmann[3], *Sergei* Karpuk[4], *Hans-Joachim* Krause[2], *Benjamin* Niederländer[4,2], *Andreas* Offenhäusser[2], *Maricel* Repetto[4], *Ulrich* Schmidt[1,a], *Lorenz* Willmann[3], and *Stefan* Zimmer[4,1]

[1] Physikalisches Institut, Ruprecht-Karls-Universität, 69120 Heidelberg, Germany
[2] Forschungszentrum Jülich, 52425 Jülich, Germany
[3] Van Swinderen Institute, University of Groningen, The Netherlands
[4] Institut für Physik, Johannes Gutenberg-Universität, 55099 Mainz, Germany

Abstract. We report on the first preliminary result of our ^{129}Xe EDM measurement performed by the MIXed collaboration. The aim of this report is to demonstrate the feasibility of a new method to set limits on nuclear EDMs by investigating the EDM of the diamagnetic ^{129}Xe atoms. In our setup, hyperpolarized ^{3}He serves as a comagnetometer needed to suppress magnetic field fluctuations. The free induction decay of the two polarized spin species is directly measured by low noise DC SQUIDs, and the weighted phase difference extracted from these measurements is used to determine a preliminary upper limit on the ^{129}Xe EDM.

1. Introduction

The Baryon asymmetry is one of the unsolved big questions of Cosmology. Most scenarios developed for explaining the Baryon asymmetry in the Universe involve modifications of the Standard Model (SM) which generate additional CP violating interactions as postulated by one of the three Sakharov criteria [1,2]. This is one reason to search for CP violating interactions beyond the SM. These CP violating interactions will also generate Electric Dipole Moments (EDM) of elementary particles, which are experimentally detectable. The search for EDMs of elementary particles is very favourable in this context because the generation of EDMs is a high order process in the SM and therefore highly suppressed. Detection of a nonzero EDM is a direct hint of new physics because SM contributions are far too small and can be neglected for all experimental searches [3,4]. For a neutral particle like the neutron, the direct EDM measurement of the free particle is a promising path, which is pursued by many collaborations. The other two elementary particles, the proton and electron, which are stable enough to perform precise EDM measurements, are charged, and Lorentz forces caused by the interaction of the charge with a magnetic field are a real obstacle for a direct EDM measurement. But bound in a neutral atom or molecule, the indirect measurement via an atomic or molecular EDM becomes feasible. The EDM of the electron can be extracted from the EDM measurement of a paramagnetic atom [5] or molecule [6], in the latter case even amplified by orders of magnitude due to molecular dipole fields. The value derived from molecular EDM measurements is rather small $d_e \leq 8.7 \cdot 10^{-29} e \cdot$ cm (90% Confidence level) [6] and progressing in the last years. For diamagnetic atoms, nuclear EDMs like the EDM of the neutron or proton induce atomic EDMs. Unfortunately these induced EDMs are reduced by Schiff screening named after Schiff's theorem [7] which states: for a nonrelativistic system made up of point charged particles which interact electrostatically with each other and with an arbitrary external field, the shielding is complete. For light nuclei, Schiff screening is perfect and prevents nuclear EDM measurements. For heavy nuclei however the nuclear EDM is not completely screened but suppressed by 2 to 3 orders of magnitude due to relativistic and finite size effects. The result of the ^{199}HgEDM $d_{Hg} \leq 7.4 \cdot 10^{-30} e \cdot$ cm (95% confidence level) [8] is the most precise limit on an EDM of diamagnetic atoms to date, providing the most stringent constraints on flavor-conserving CP violating phases. This upper limits of the ^{199}HgEDM also give the best indirect constraints on the proton EDM $d_p \leq 2.0 \cdot 10^{-25} e \cdot$ cm [9] and on the neutron EDM $d_n \leq 1.6 \cdot 10^{-26} e \cdot$ cm [10], whereas from direct neutron EDM searches the present upper limit is $d_n \leq 2.0 \cdot 10^{-26} e \cdot$ cm [11]. This example shows that the high measurement precision achieved in diamagnetic atom EDM measurements can provide severe constraints on CP violation in purely hadronic interactions in spite of the fact that Schiff screening reduces the EDM sensitivity by 2 to 3 orders of magnitude.

Investigating the ^{129}Xe EDM is a different approach to improve the EDM sensitivity in the hadronic sector. Technically, our measurement sensitivity benefits from the extraordinary long spin coherence times that can be achieved under dedicated experimental conditions (for further details see [12]).

2. Setup

In our setup (Fig. 1) we directly measure the free induction decay of transversal nuclear polarized ^{3}He and ^{129}Xe atoms by means of Superconducting Quantum Interference

[a] e-mail: ulrich.schmidt@physi.uni-heidelberg.de

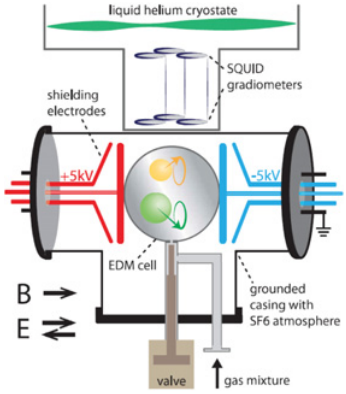

Figure 1. Inner part of the MIXed ^{129}Xe-EDM experiment.

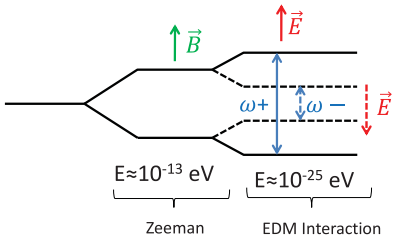

Figure 2. Level scheme ^{129}Xe-EDM.

Devices (SQUIDs) in a gradiometer configuration. The low noise DC SQUIDs are housed in a metal free fibre glass cryostat to maintain them on their operating temperature of about 4 K. The gradiometer configuration enables us to operate the SQUIDs in a 400 nT magnetic field with a resolution of a few fT/$\sqrt{\text{Hz}}$, limited by noise. Not only within the cryostat, but also within the whole setup close to the SQUIDs and the EDM cell we avoid any metal, because the Johnson noise of the free moving electrons inside a metal would induce severe magnetic noise in our SQUIDs. Below the cryostat, the housing of the EDM cell is mounted which is made of glass, covered by a slightly conductive layer to avoid charge up. The EDM cell of 10 cm diameter is placed between high voltage electrodes which provide an electrical field of 800 V/cm strength with switchable polarity. We use a very moderate high voltage for this setup in order to be on the safe side concerning sparks and leakage currents. Below the EDM cell, a pressurized air controlled valve allows for filling the EDM cell from outside.

As shown in the level scheme of a ^{129}Xe-atom inside a homogenous magnetic holding field of 400 nT (Fig. 2), the energy shift caused by a hypothetical EDM is about 12 orders of magnitude smaller than the Zeeman splitting of the holding field. Therefore comagnetometry is mandatory in order to get rid of magnetic field drifts. Here the co-located nuclear polarized ^{3}He atoms serve as an ideal magnetometer because any possible interaction of the electrical field with an EDM from the ^{3}He nucleus is completely suppressed by Schiff screening. Technically we have to measure the ^{129}Xe frequency relative to the ^{3}He frequency. We achieve this by calculating the frequency difference weighted by the gyromagnetic ratio of the two nuclear spin species.

$$\Delta\omega = \omega_{Xe} - \frac{\gamma_{Xe}}{\gamma_{He}}\omega_{He}, \quad \text{with} \quad \frac{\gamma_{Xe}}{\gamma_{He}} \approx 0.363 \qquad (1)$$

While frequency shifts caused by magnetic field drifts are cancelled in the frequency difference $\Delta\omega$, shifts due to a hypothetical ^{129}Xe-EDM interaction with the electrical field are still present. For practical reasons we evaluate Eq. (1), which is the integrated form of (1) over time. For an EDM below the sensitivity of our experiment, the phase $\Delta\Phi$ should be constant.

$$\Delta\Phi = \Phi_{Xe} - \frac{\gamma_{Xe}}{\gamma_{He}}\Phi_{He} = const \qquad (2)$$

A closer look on Eq. (2) reveals further corrections, as shown in Eq. (3) besides the phase shift $\Phi(t)_{EDM}$ caused by a nonzero EDM. The most prominent one in our case is earth rotation (coefficient a_{lin}). During the course of one day, we accumulate an additional phase of 60% of 2π because we are in a rotating frame (i.e., the detector rotates around the precessing spin sample). Furthermore, the chemical shift, dependent on the partial pressures of all gas species inside the measurement cell including buffer gases, affects the effective value of the gyromagnetic ratio on the order of 10^{-7}. Both effects contribute to the linear correction term a_{lin} which we treat as a free parameter because we cannot calculate the chemical shift precisely enough (absolute order 10^{-10}). Finally we have to correct for the general Ramsey-Bloch-Siegert-shift which consist of two components. One is caused by the self interaction of the spin species (coefficient a_{He} and a_{Xe}) within the given magnetic field, while the other follows from the interaction between two different spin species, which we called cross talk (coefficient b_{He} and b_{Xe}).

$$\begin{aligned}\Delta\Phi = {} & c + a_{lin}\cdot t \\ & + a_{He}\cdot e^{-t/T^*_{2,He}} + a_{Xe}\cdot e^{-t/T^*_{2,Xe}} \\ & + b_{He}\cdot e^{-2t/T^*_{2,He}} + b_{Xe}\cdot e^{-2t/T^*_{2,Xe}} \\ & + \Phi_{\text{EDM}}(t)\end{aligned} \qquad (3)$$

The cross talk is an analogue of the classical Bloch-Siegert-shift in NMR. Here this shift is caused by the tiny magnetization of the other spin species precessing with a different frequency in contrast to the case of classical NMR where this shift is caused by the counter propagating component of the linear RF-field. As in the case of NMR this shift depends quadratically on the magnetization amplitude ($\sim e^{-2t/T^*_2}$). Because of the unavoidable presence of magnetic field gradients, the Larmor frequency is slightly different in different parts of the gas cell. A first order approximation following Ramsey's paper [13] leads to a frequency shift depending linear on the magnetization amplitude ($\sim e^{-t/T^*_2}$) of the same spin species.

Therefore the functional dependence on time of all correction as shown in Eq. (2) is well known, and the parameters, in this case the relaxation times $T^*_{2,He}$ of ^{3}He and $T^*_{2,Xe}$ of ^{129}Xe are well determined by fitting exponential functions to the measured decaying amplitudes of the SQUID signal shown in Fig. 4. However, we cannot determine the amplitudes of these phase corrections well enough by independent measurements. Therefore we include the amplitudes (Eq. (2): $a_{He}, a_{Xe}, b_{He}, b_{Xe}$) of the generalized Ramsey-Bloch-Siegert-shift as free parameters in a global fit

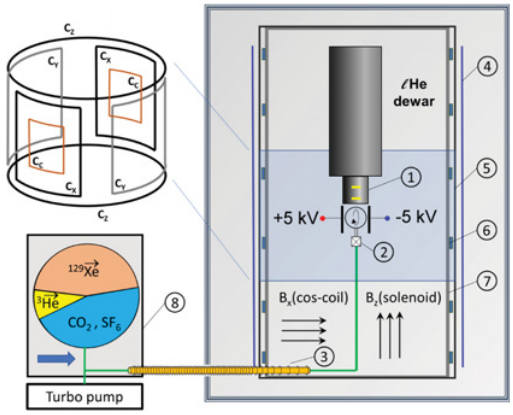

Figure 3. Setup of the MIXed ^{129}Xe-EDM experiment. The central part of the experiment, i.e. the SQUID-gradiometer (1) and the EDM cell (2), is placed inside a two-layer magnetically shielded room (MSR) with an additional mu-metal cylinder (4) to reduce magnetic field gradients. A coil system consisting of a cosine-coil (5) and a solenoid (6) generates a homogeneous magnetic guiding field. Four additional shimming, coils (shown in the top-left corner) are used to compensate gradients. A fibre-reinforced plastic tube (7) acts a rigid mounting structure for all components inside the MSR. The gas mixture of hyperpolarized ^{3}He and ^{129}Xe, and buffer gases is prepared outside the MSR (8) and then transferred through filling lines equipped with solenoids (3) to the EDM cell.

together with a parameter for a linear shift (a_{lin}) which accounts for earth rotation and the chemical shift as already discussed above. The raw data from the SQUID gradiometers (Fig. 1) sampled with 250 Hz are divided in sub cuts of 4 second duration. Then these sub cuts are fitted with sin and cos functions of the corresponding frequency. From the coefficients of the sin and cos functions, we calculate the average amplitudes and phases of ^{3}He and ^{129}Xe with the corresponding errors for each sub cut. Further details of these corrections and how we perform the whole data analysis can be found in [14].

The whole setup, located at the Research Center Jülich, is shown in Fig. 3. Inside a double layer magnetically shielded room, we placed a µ-metal cylinder 85 cm in diameter, 1.9 m in height to provide additional magnetic shielding from outside. The main task is to reduce magnetic field gradients from 300 pT/cm to 50 pT/cm. The µ-metal cylinder also serves as a return yoke for the cos-coil, which generates a very homogeneous horizontal magnetic field. A magnetic field along the cylinder axis is generated by a set of solenoids optimized for field homogeneity.

In order to reach long transverse relaxation times, it is necessary to further minimize the magnetic field gradients actively. In the past we already used free induction decay time T_2^* measurements to determine small magnetic field gradients [15]. Here we employ T_2^* measurements as the control element in a feedback loop. This was achieved by additional shimming coils that produce inhomogeneous fields, consisting of Anti-Helmholtz coils along the cylinder axis, and saddle coils perpendicular to the cylinder axis to compensate magnetic field gradients shown in the left upper part of Fig. 3. The following online method is used: The EDM cell is filled with ca. 30 mbar of hyperpolarized ^{3}He aligned

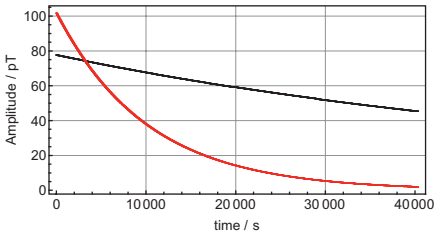

Figure 4. Free induction decay (run number 4) of ^{3}He (black) and ^{129}Xe (red). The error bars are so small and the points are so dense that it looks like continuous lines.

with the magnetic field. After a non-adiabatic $\pi/2$ spin flip, the Larmor precession signal is monitored. The transverse relaxation time of Helium is maximized by systematically varying the coil currents according to a downhill simplex algorithm. For each setting of coil currents, the transverse relaxation time T_2^* is measured for several minutes. The fully automated optimization procedure takes approximately twelve hours, improving the transverse relaxation time T_2^* from 7500 s to 40000 s (see Fig. 4). This corresponds to a reduction of magnetic field gradients from 50 pT/cm to below 10 pT/cm. This method has the advantage that an EDM measurement run can directly follow the gradient optimization procedure without any modifications of the setup. The individual steps to perform a single EDM measurement run are: A gas mixture of hyperpolarized ^{3}He and ^{129}Xe and buffer gases is prepared outside the MSR. The solenoids of the filling line are switched on, as well as the cos-coil which serves as a guiding field in the x-direction. The gas mixture expands through the filling lines into the evacuated EDM cell. The solenoids of the filling line are ramped down; and the magnetic guiding field of the EDM setup slowly rotates into the z-direction by decreasing the current through the cos-coil and simultaneously increasing the current through the solenoid. A non-adiabatic $\pi/2$ spin-flip back to the xdirection starts the spin precession. Then the electric field is ramped up and regularly inverted. The signal of the precessing magnetization is monitored by low-temperature SQUIDs (very sensitive, low-noise magnetometers) and recorded for off-line evaluation. The individual He and Xe phases are extracted from the data, and the weighted phase difference is calculated as explained above.

3. Results

In one week of measurement time, we were able to perform 6 data taking runs (about 10 hours each) after shimming of the field gradients. Each run was subdivided into sub cuts of 4 second duration, and we follow the procedure described above. Figure 5 shows the resulting phase difference $\Delta\Phi$ for run number 4 after applying different types of corrections. The upper part shows the phase difference after correcting the linear phase shift due to earth rotation and the chemical shift (coefficient c, a_{lin} of Eq. (2)). Because we analyse the phase difference $\Delta\Phi$, the periodical switching of the electrical field direction will result in a triangular shaped phase shift versus time as shown in Fig. 5 lower part for a hypothetical EDM of $d_{Xe} = 4.0 \cdot 10^{-25} e \cdot \mathrm{cm}(\Phi_{\mathrm{EDM}}(t)$ term in Eq. (2)). The middle part shows the residual resulting from fitting. Because of the decaying amplitude mainly of the Xe (see

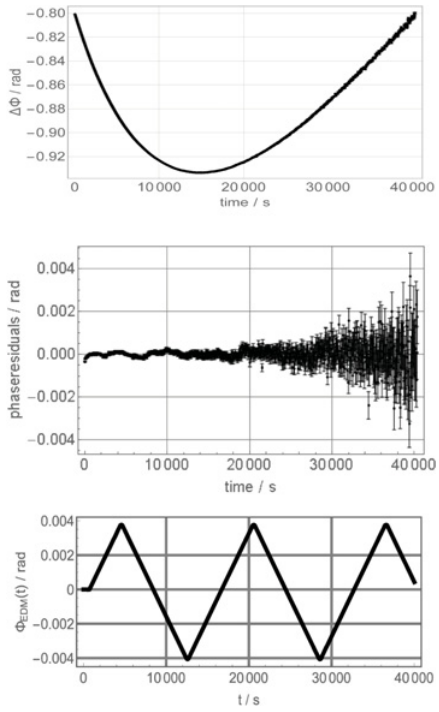

Figure 5. For run number 4; upper part: phase difference $\Delta\Phi$ after correction for earth rotation and chemical shift, middle part: residual phase difference $\Delta\Phi$ after the correction for the generalized Ramsey-Bloch-Siegert-shift, lower part: hypothetical EDM signal $\Phi_{\mathrm{EDM}}(t)$ for $d_{Xe} = 4.0 \cdot 10^{-25} e \cdot$ cm.

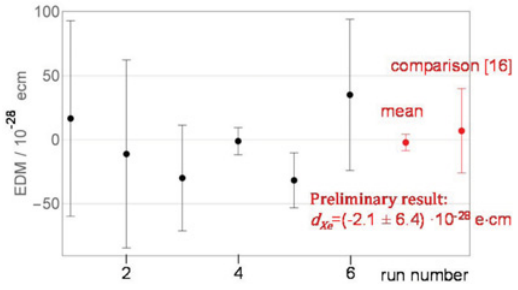

Figure 6. EDM values of different runs.

Fig. 4), the signal-to-noise ratio becomes worse with time which leads to increasing error bars. From fitting this function simultaneously with all corrections to the phase shift (Eq. (2)), we can determine an EDM value together with the corresponding error. For all runs, this EDM value is shown in Fig. 6. These EDM-runs also served to optimize the parameter settings, i.e. the respective partial pressures of the He, Xe and buffer gases under the given gradient conditions and T_1 relaxations times in the EDM cell. It also depends on the actual system noise. The strong fluctuations of the error bars of the individual runs indicate these highly delicate dependencies and show, that we still in the phase of parameter optimization. Together with the values of the individual runs, the preliminary result and the 1σ error for the mean over all 6 runs is shown. The result is in concordance with zero. For comparison, the world's best upper limit on an atomic EDM [16] is also shown. In order to get a final result, two points are still missing. According to the standards of high energy physics, we should verify the correctness of our fitter and the implemented method in combination with our model

Table 1. Upper limit systematic effects.

Upper limit systematic effect	Value / e·cm
Leakage currents	$4{\cdot}10^{-32}$
Magn. field during polarity reversal	$2{\cdot}10^{-32}$
Motional magn. field	$5{\cdot}10^{-37}$
Geometric phase effect	$7{\cdot}10^{-30}$
Ramsey-Bloch-Siegert shift	$8{\cdot}10^{-30}$
Total	$2{\cdot}10^{-29}$

Table 2. Improvements we aim for within the next 5 years.

Improvement	Factor
Increase the electric field strength (now: E=800 V/cm)	4 to 5
Increase Xe and He partial pressure (trade-off between signal strength and spin coherence time)	2
New magnetically shielded room at Heidelberg improves noise level	10
Increase measurement time from 2 days to 200 days	10

either by evaluating several (more than ten) Monte Carlo simulated data set and get the same results, as it was put into the simulations, or evaluate with an independent method. The correctness of the fitter implementation was already tested by two independent implementations at Heidelberg (Mathematica) and Groningen (Python). Because some of us have to do this job for other experiments as well, we decided to follow the second option. In addition to our classical Frequentist analysis (result Fig. 6), we are performing a Bayesian analysis employing Markov chain Monte Carlo calculation for integrating over all nuisance parameters. This additional analysis is finished soon. Further we investigate the electrical field strength inside our spherical cell by optical methods under the conditions that we run the experiments. The final results of these investigations are also in reach. With respect to the electrical field distribution, a cylindrical cell has the preferred shape. We use a spherical cell for our measurements because for a cylindrical cell, additional phase shifts to the ones shown in Eq. (2) arise due to demagnetization effects of the magnetized sample itself. We were not able to get these additional phases shift under control in a deterministic way, so we changed our setup to run with a spherical cell.

Furthermore we investigate other possible sources of false effects of the EDM signal listed in Table 1 where one major contribution at the present sensitivity level comes from geometric phase effects which are discussed in detail in [17]. The second major contribution, the Ramsey-Bloch-Siegert shift, is a consequence of the approximation we used.

4. Conclusion and Outlook

Our result shows that our method, measuring the free induction decay of co-located spin species with low noise DC SQUIDs, is competitive to other methods like maser

techniques [16] in setting lower upper limits for the ^{129}Xe EDM. Because our first approach was in some aspects not yet fully optimized, improvements of our setup are possible, as shown in Table 2. This improvement by 2 to 3 orders of magnitude is necessary to become competitive to the ^{199}Hg EDM and to bolster the search for a proton EDM where the relative sensitivity of the ^{129}Xe is higher.

Besides establishing lower limits for the ^{129}Xe-EDM, we will also use our setup with slight modifications to search for axion like dark matter and for Lorentz invariance violations, as we did in the past [14].

References

[1] A. Sacharow, ZhETF Pis'ma **5**, 32 (1967a)
[2] A. Sacharow, JETP Letters **5**, 24 (1967b)
[3] I.B. Khriplovich, PLB **173**, 193 (1986)
[4] M. Pospelov, A. Ritz, Phys. Rev. D **89**, 056006 (2014)
[5] E. D. Commins, S. B. Ross, D. DeMille, B.C. Regan, Phys. Rev. A **50**, 2960 (1994)
[6] V. Andreev et al., ACME collaboration, Nature **562**, 355 (2018)
[7] L. I. Schiff, Phys. Rev. **132**, 2194 (1963)
[8] B. Graner, Y. Chen, E.G. Lindahl, B.R. Heckel, Phys. Rev. Lett. **119**, 119901 (2017)
[9] V.F. Dmitriev, R.A. Sen'kov, Phys. Rev. Lett. **91**, 212303 (2003)
[10] B. Graner, Y. Chen, E.G. Lindahl, B.R. Heckel, arXiv:1601.04339v4 (2017)
[11] J.M. Pendlebury et al., Phys. Rev. D **92**, 092003 (2015)
[12] T.E. Chupp, P. Fierlinger, M.J. Ramsey-Musolf, J.T. Singh, Rev. Mod. Phys. **91**, 015001 (2019) [arXiv:1710.02504v2]
[13] N.F. Ramsey, Phys. Rev. **100**, 1191 (1955)
[14] F. Allmendinger et al., Phys. Rev. Lett **112**, 110801 1-5 (2014)
[15] F. Allmendinger et al., Eur. Phys. J. D. **71**, 98 (2017)
[16] M.A. Rosenberry, T.E. Chupp, Phys. Rev. Lett. **86**, 22–25 (2001)
[17] J.M. Pendlebury et al., Phys. Rev. A **70**, 032102 (2004)